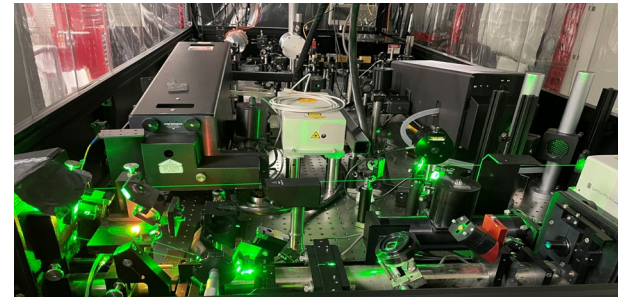
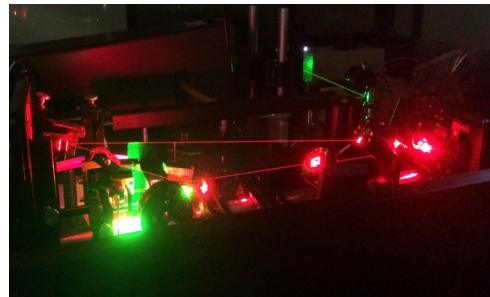
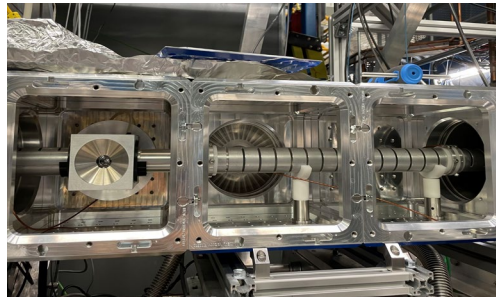
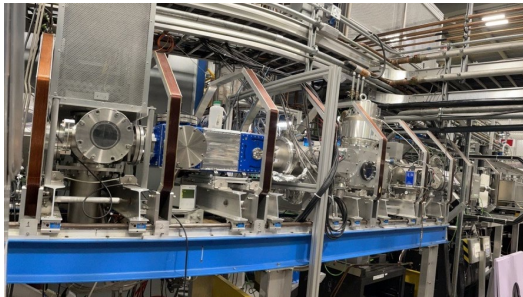


nuclear spin polarization & collinear laser spectroscopy program at TRIUMF

Ruohong Li

on behalf of Targets & Ion Sources – Laser Applications group

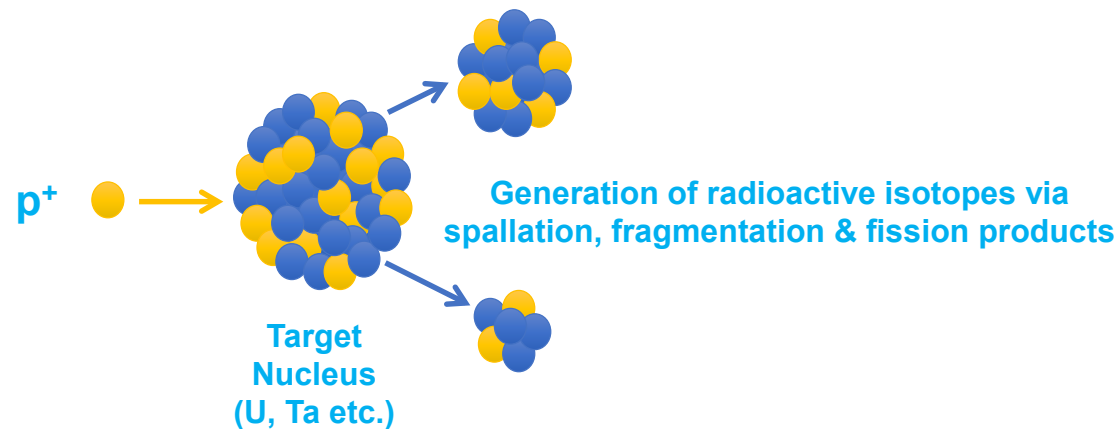
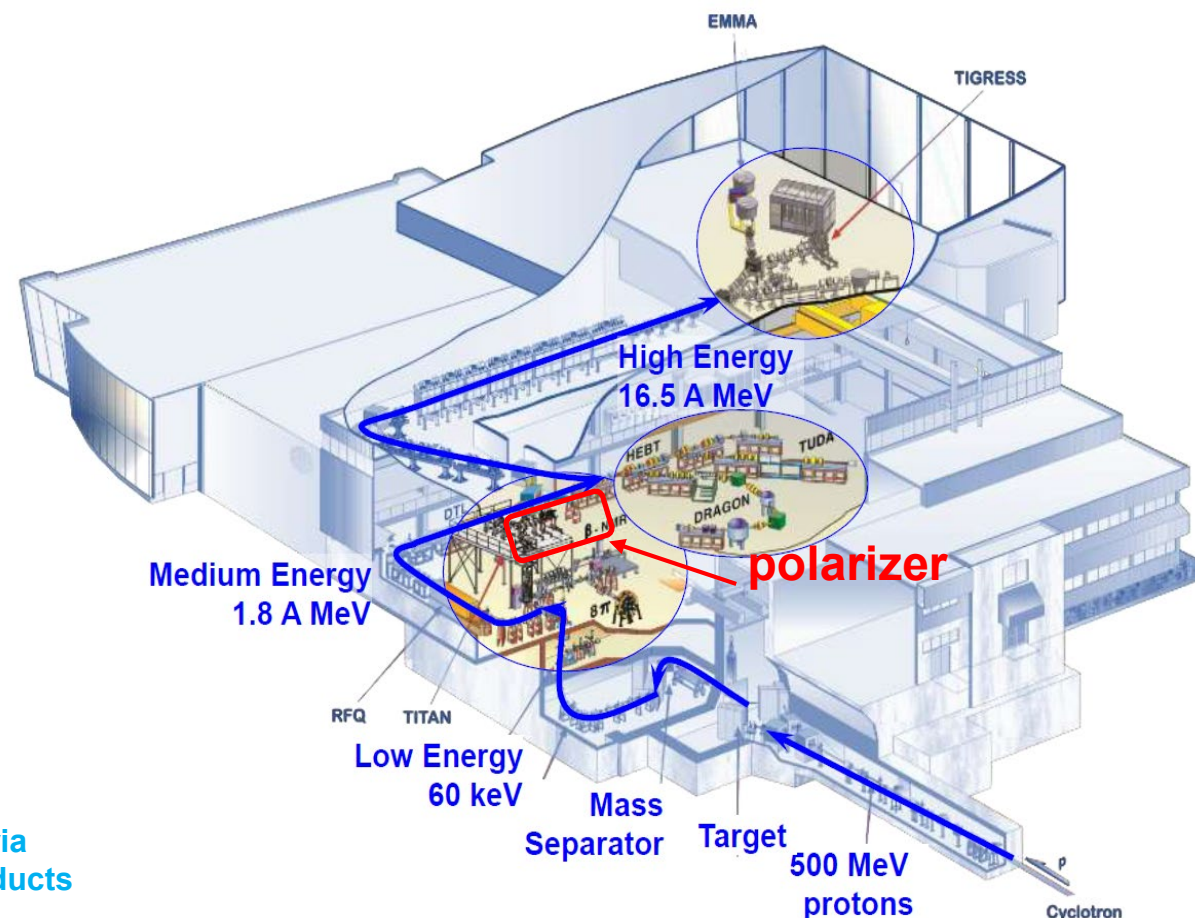
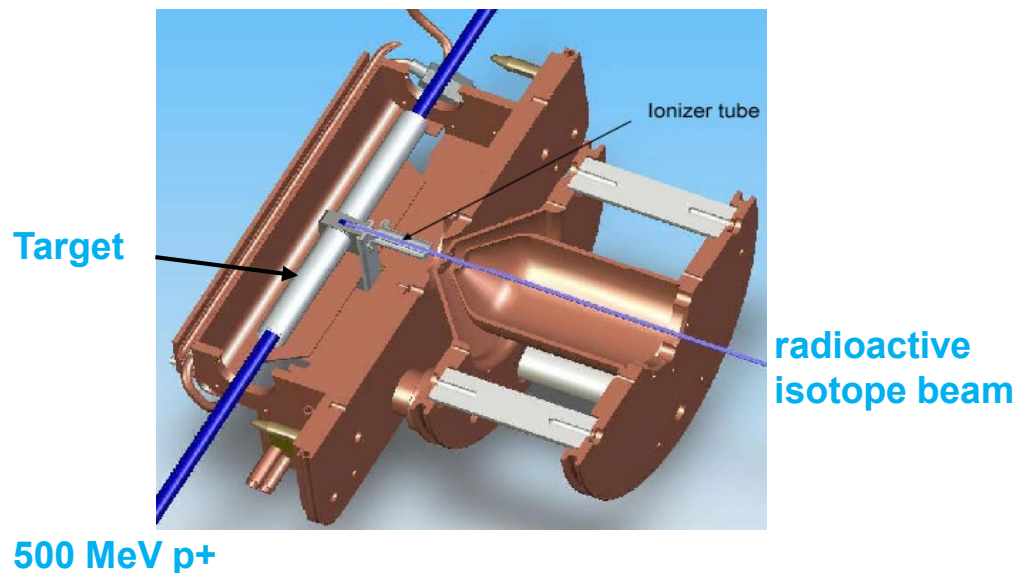




- **TRIUMF** founded 1968 by SFU, UBC and U Victoria (**TRI**-University **M**eson **F**acility).
- TRIUMF has world's largest cyclotron (**520** MeV, **18-meter** diameter).
- Has **20** Canadian member universities and works with **50** foreign institutions in **30** different countries.
- staffed by **350** scientists, engineers, technicians, and **150** postdoc's, graduate- and co-op- students.

Use radioactive isotopes to study nuclear physics, astrophysics, material science and life science

3



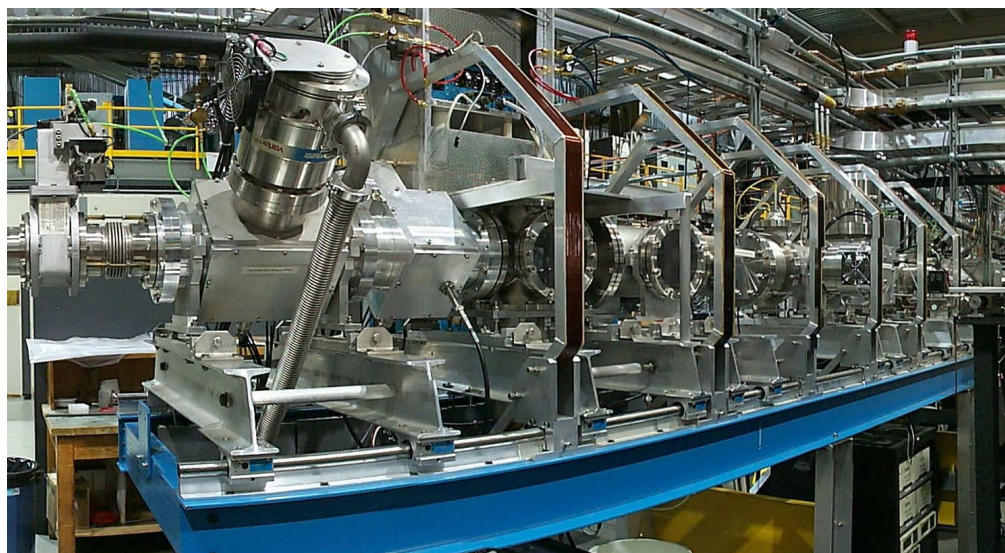
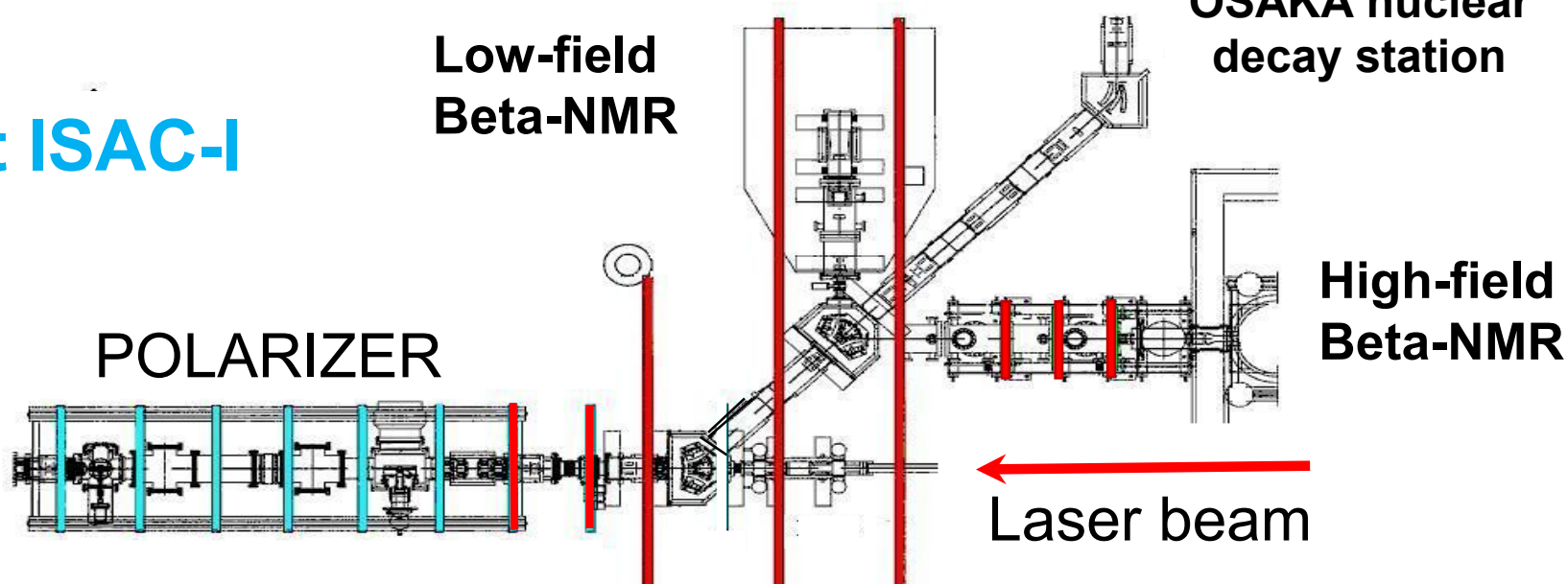
cyclotron
p⁺ @ 480 MeV and up to 100μA to ISAC



Discovery,
accelerated

polarizer facility at ISAC-I

Low energy
radioactive ion beam

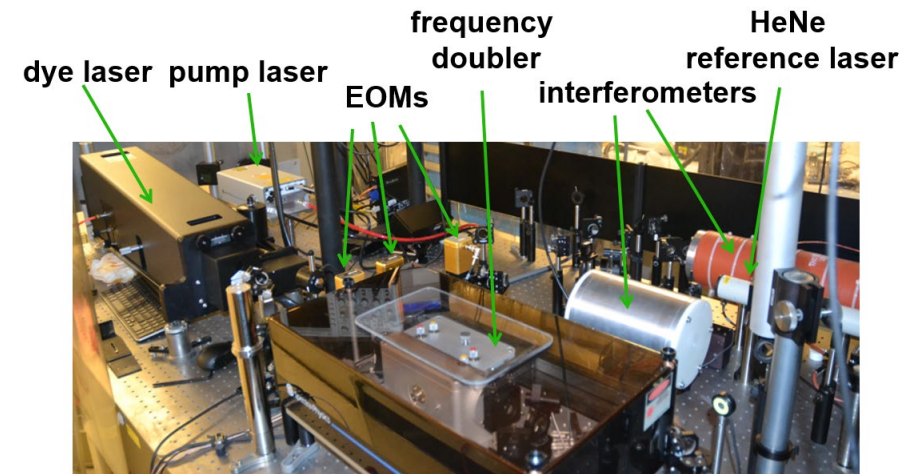
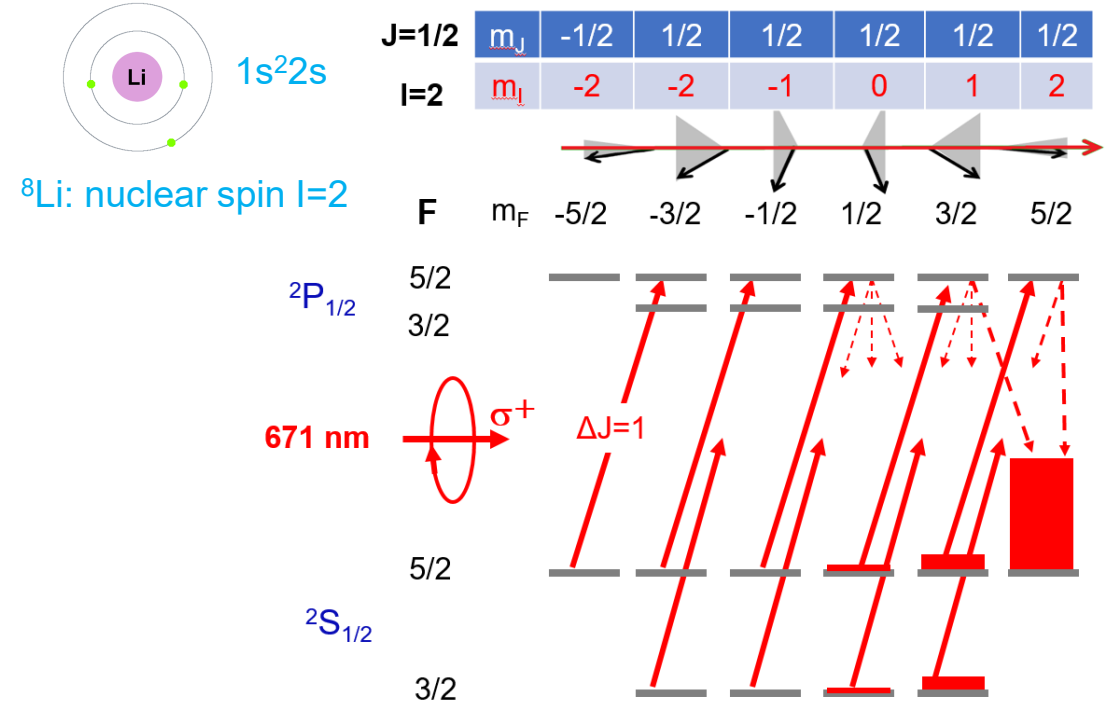
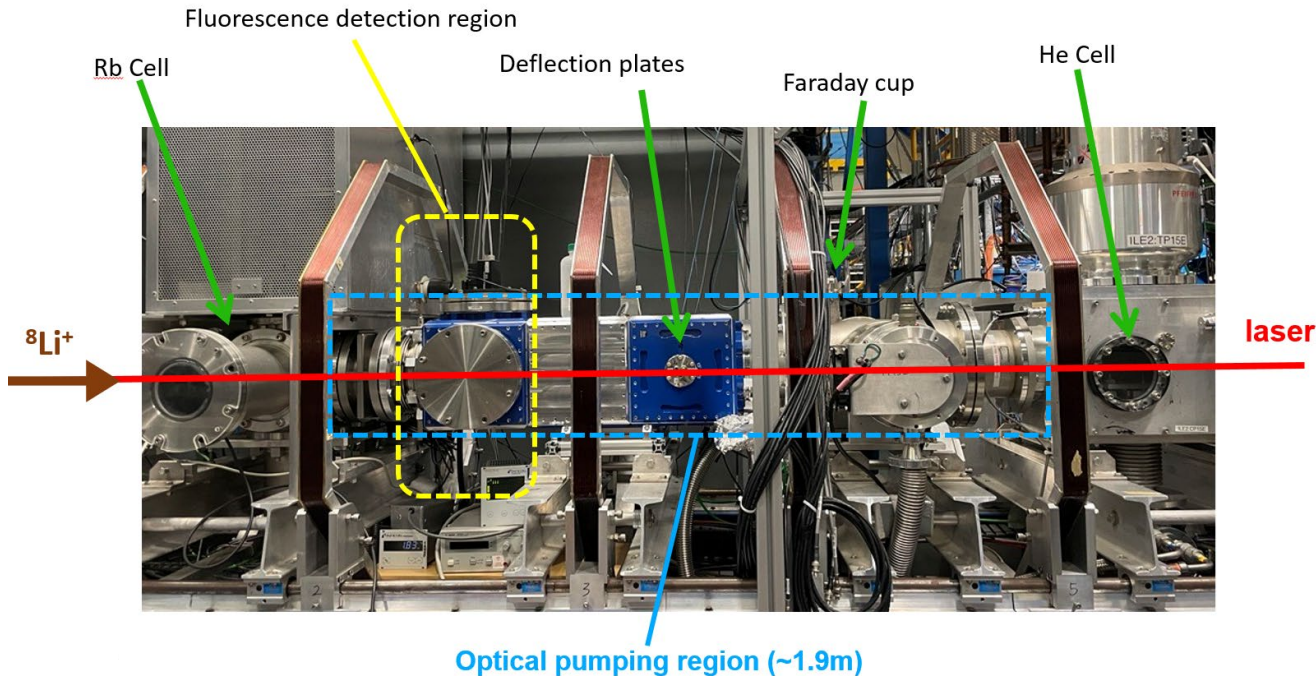
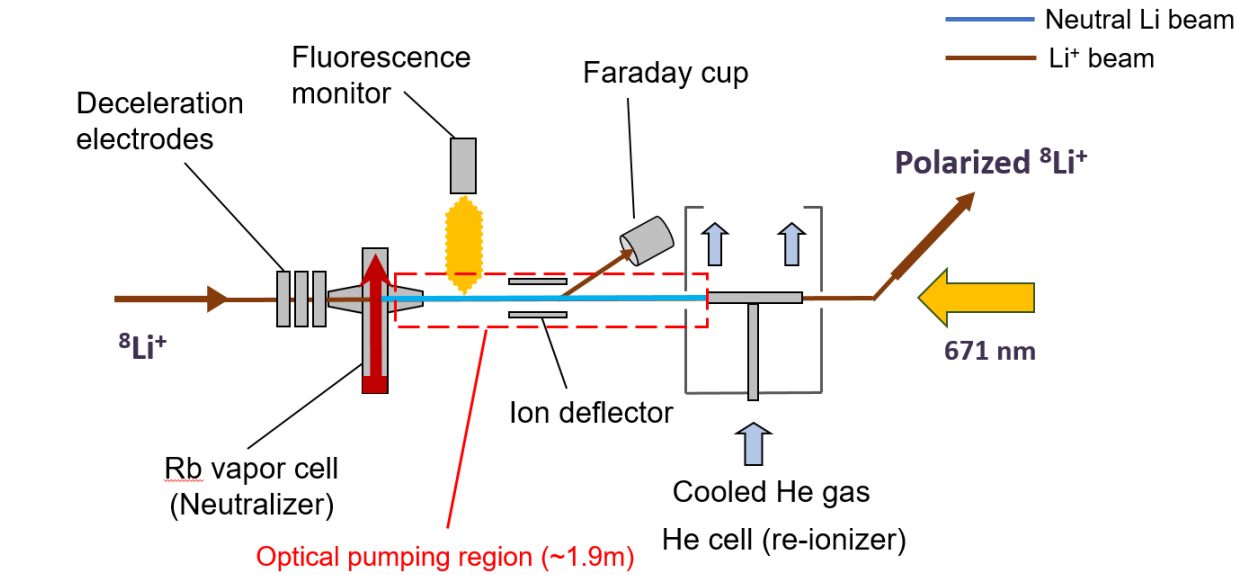


functions: provide **hyperf polarized** (polarization up to 90%) radioactive nuclei **~800 hours/year** for scientific research: beta-detected nuclear magnetic resonance (β -NMR) for material-, life-science, nuclear physics, and fundamental symmetries.

method: collinear **optical pumping** using lasers

nuclear-polarized beams:

- ^8Li , ^{31}Mg (routine delivery), ^{33}Mg (new 2023)
- $^{230, 232}\text{Ac}$, $^{58, 74}\text{Cu}$, ^{32}Na etc. (in development)



- different isotopes have different isotope shift (IS) and hyperfine structures (HFS). To manipulate the electron population within these structures, dedicated laser system need to be purchased/developed.

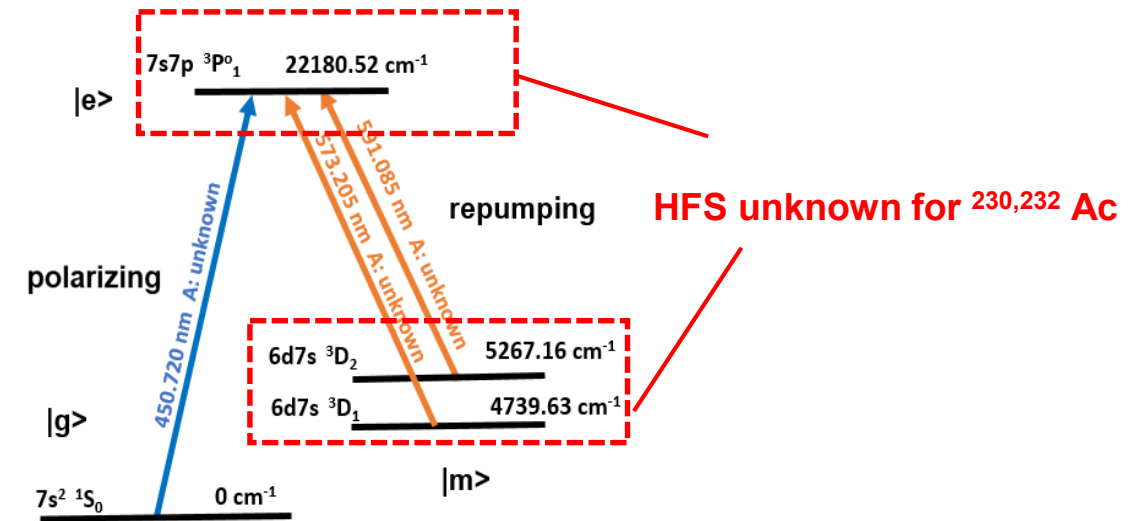
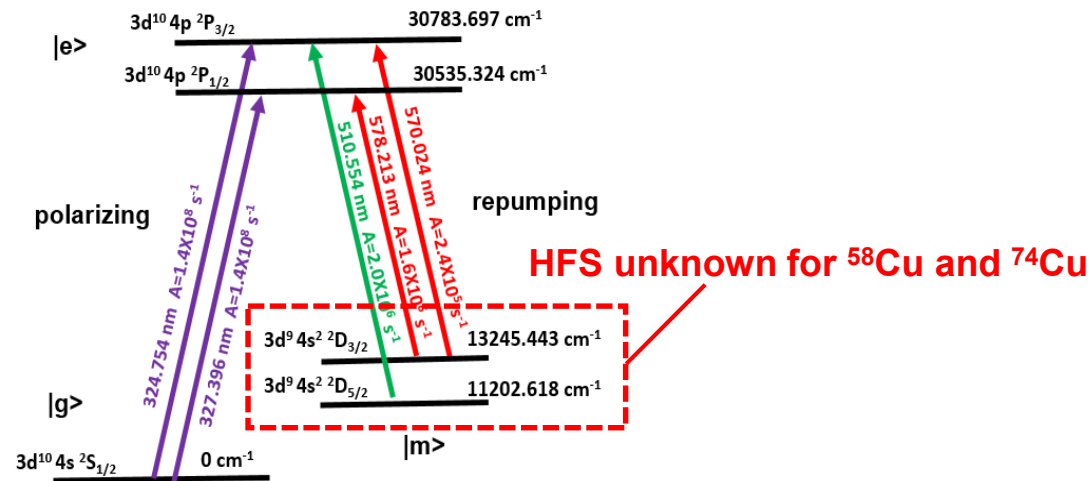
6



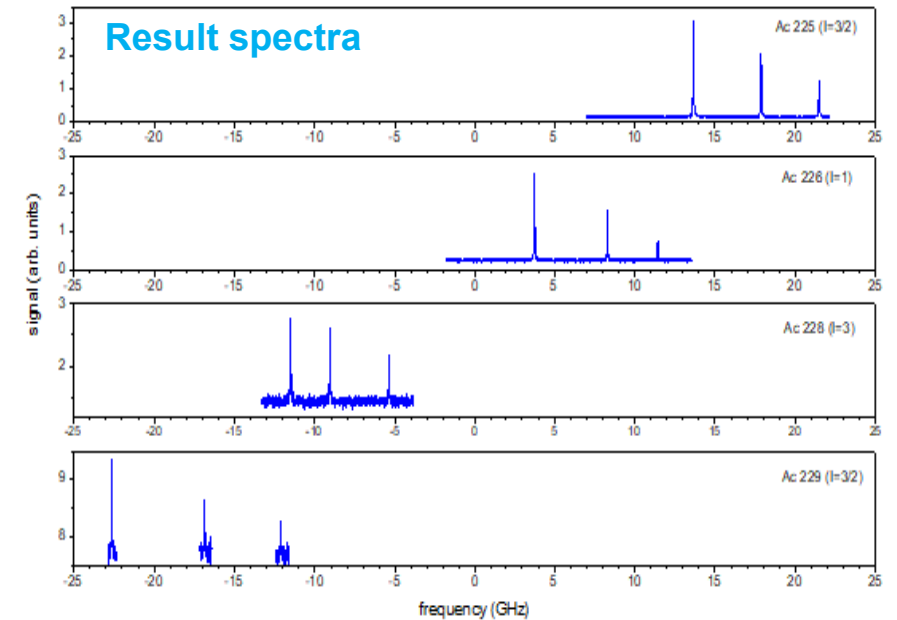
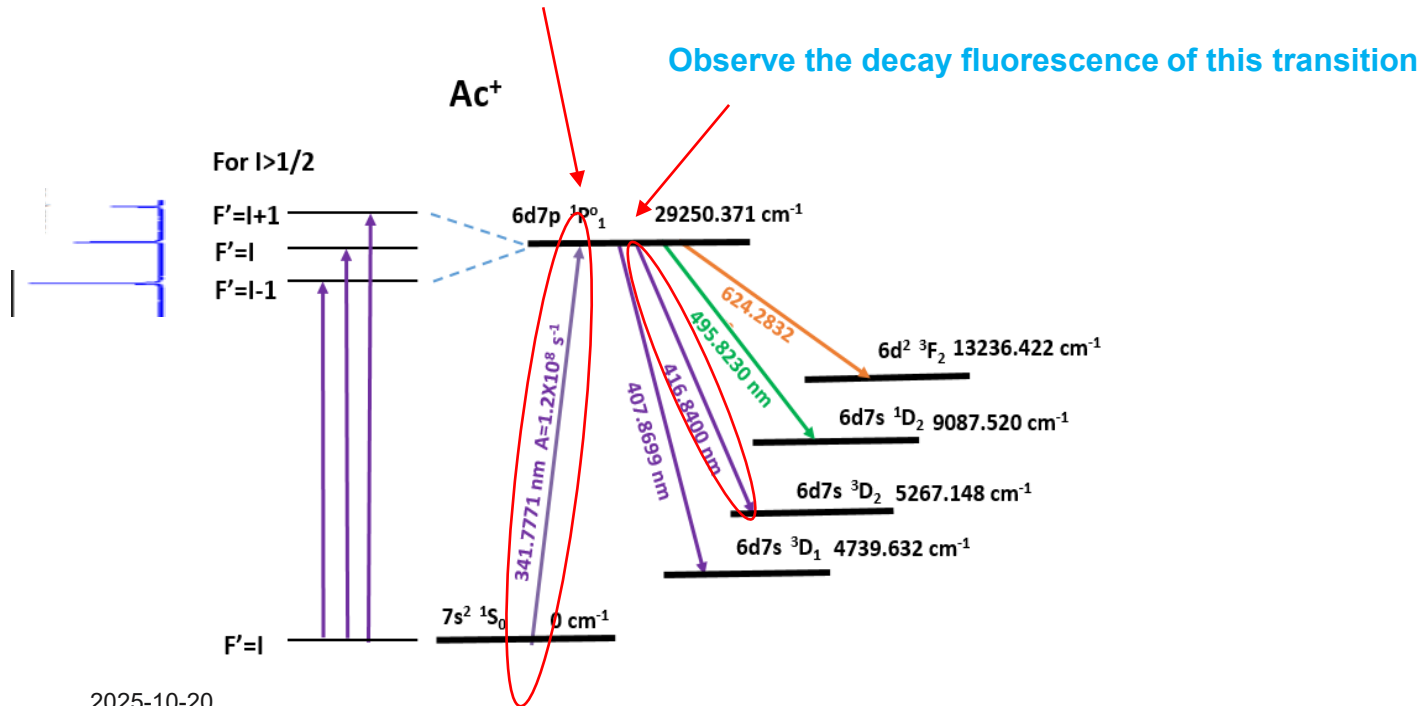
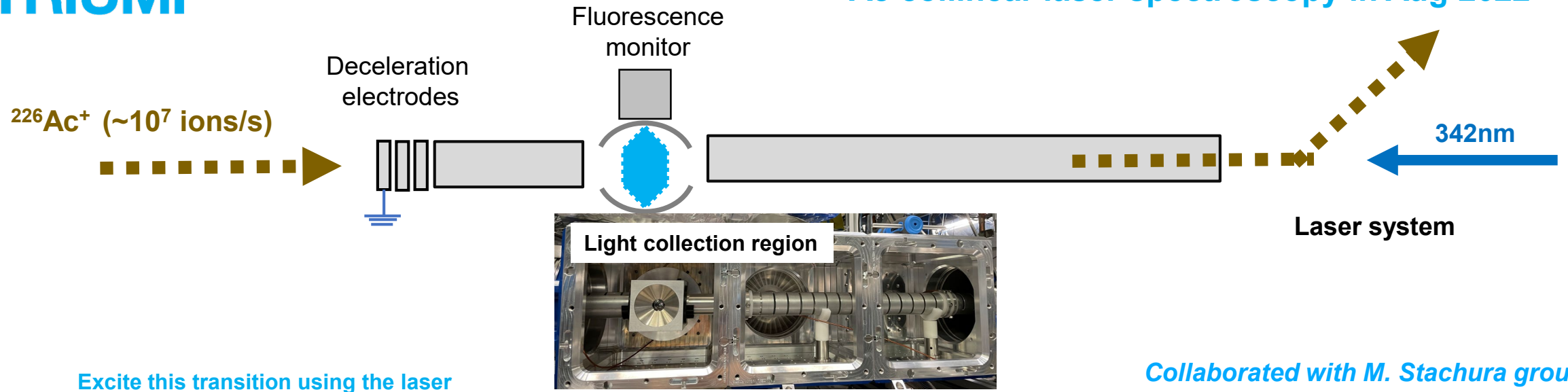
Alzheimer's disease



^{225}Ac highly promising for targeted alpha cancer therapy



- difficult wavelength regions: blue or UV which needs frequency doubling
- multiple lasers & modulators needed for pumping and re-pumping the electronic population
- for some isotopes, such as ^{58}Cu , ^{74}Cu , and $^{230,232}\text{Ac}$, hyperfine structures are unknown.
→collinear spectroscopy to be done before attempting laser polarization.



For ^{230}Ac and ^{232}Ac , we could not get the spectra due to the **low production rate $<10^4/\text{s}$** and limited time

High-resolution spectra of $^{225}, ^{226}, ^{228}, ^{229}\text{Ac}$

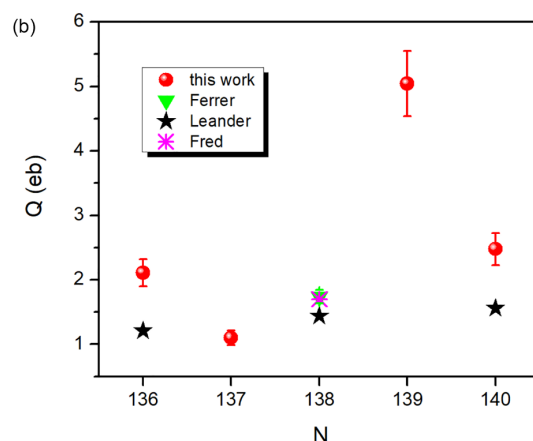
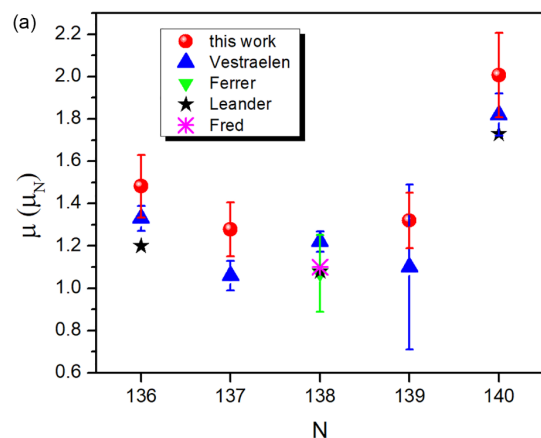
linewidth: $\sim 40\text{MHz}$
resolved hyperfine structure

➔ extracted hyperfine constants and isotope shift

nuclear properties can be further extracted:

- change of charge radii $\delta\langle r^2 \rangle$
- nuclear magnetic dipole moment μ
- nuclear electric quadrupole moment Q

measured μ and Q (first time) of $^{225}, ^{226}, ^{228}, ^{229}\text{Ac}$

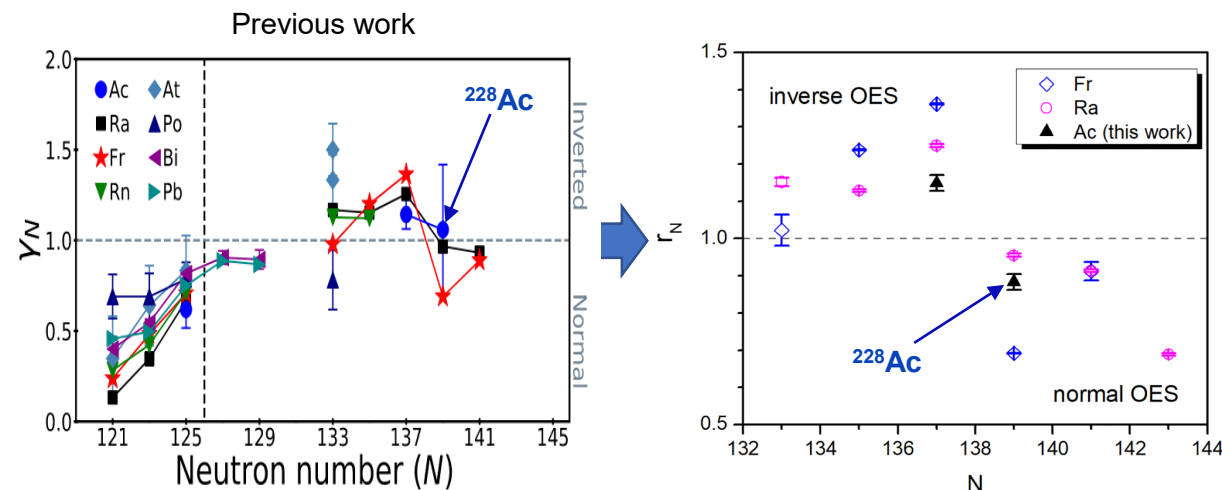


Collinear laser spectroscopy on neutron-rich actinium isotopes

Ruohong Li^{1,2,3,*}, Andrea Teigelhöfer¹, Jiguang Li^{4,†}, Jacek Bieroń⁵, András Gácsbaranyi^{1,‡}, Jake Johnson⁶, Per Jönsson⁷, Victoria Karner¹, Mingxuan Ma⁴, Martin Radulov¹, Mathias Roman¹, Monika Stachura¹, and Jens Lassen^{1,8,9}

High-resolution collinear laser spectroscopy of neutron-rich actinium has been performed at TRIUMF's isotope separator and accelerator facility ISAC. By probing the $7s^2 \ ^1S_0 \rightarrow 6d7p \ ^1P_1$ ionic transition, the hyperfine structures and optical isotope shifts in $^{225,226,228,229}\text{Ac}^+$ have been measured. This allows precise determinations of the changes in mean-square charge radii, magnetic dipole moments, and electric quadrupole moments of these actinium isotopes. The improved precision of charge radii and magnetic moments clears the ambiguity in the odd-even staggering from previous studies. The electric quadrupole moments of $^{225,226,228,229}\text{Ac}$ are determined for the first time.

Determine the clear boundary of inverse OES



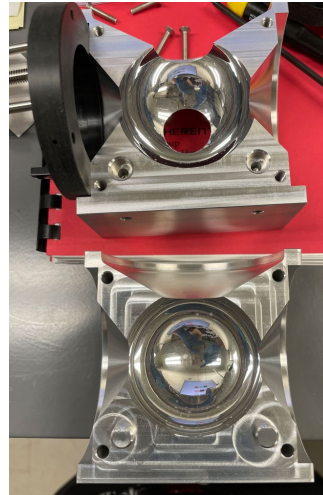
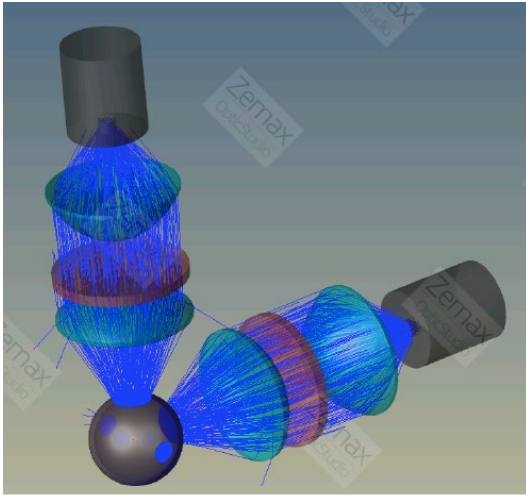
How to improve our detection efficiency?

To polarize exotic isotopes with low production rates: e.g. ^{230}Ac ($<10^4/\text{s}$), ^{32}Na ($\sim 100/\text{s}$)), CLS is required to determine relevant HFS and IS

9

Improve the fluorescence detection system

Spherical mirror system designed by OSAKA/TRIUMF
(used for Ac^+ CLS experiment online in 2022)



collection eff:
11% one axis
22% two axes
combined

Improve on photomultiplier tube: bigger PMT detection area
higher quantum efficiency
lower dark counts

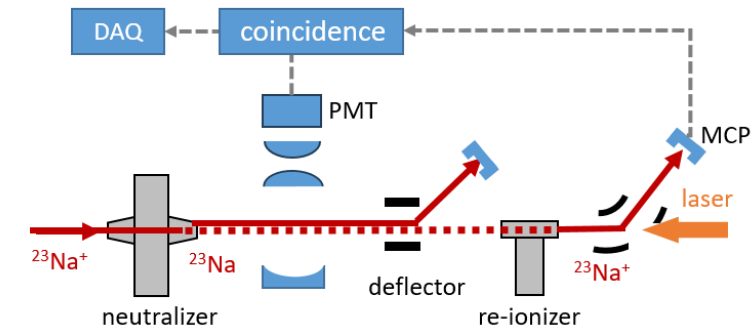
^{23}Na stable beam test in 2017 and 2023:

total detection efficiency is $5\text{-}15 \times 10^{-5}$

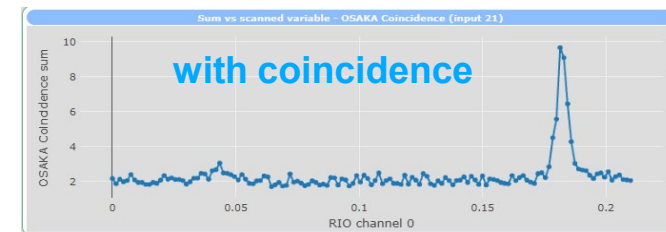
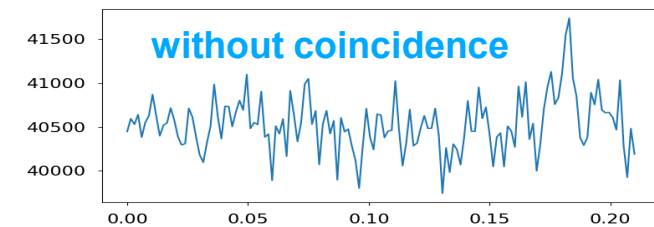
Developing is continuing

Photon-ion coincidence method

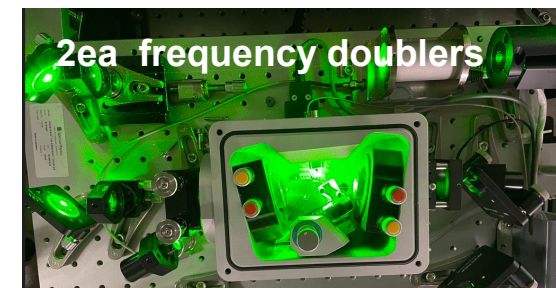
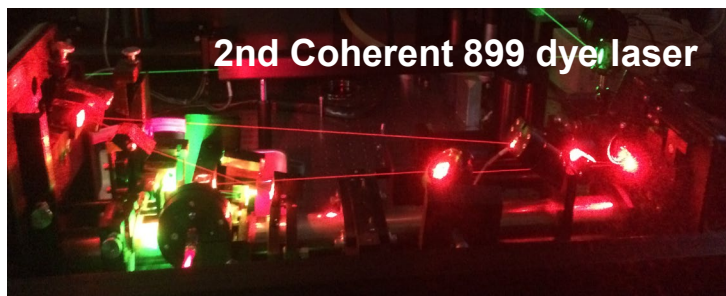
^{23}Na stable beam test in 2023 with OSAKA group



$^{23}\text{Na} \sim 2 \times 10^4/\text{s}$

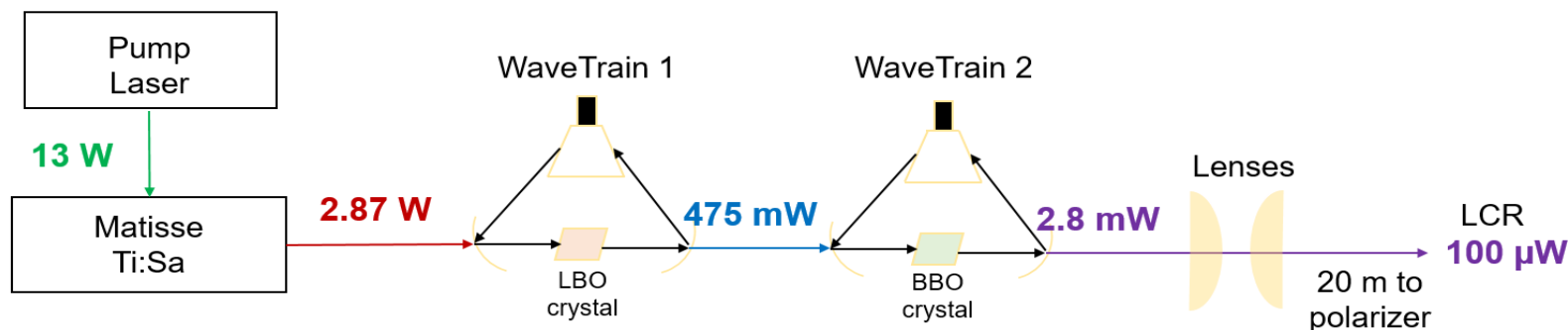


upgraded laser systems for polarized beams & collinear laser spectroscopy

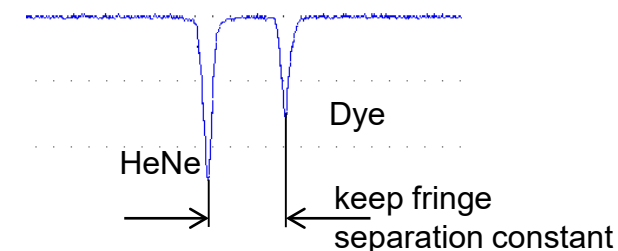


- 2nd coherent 899 dye lasers + frequency doubler + fringe offset lock
- 1ea Matisse CS Ti:Sa laser + 1ea frequency doubler + 1ea fringe offset lock

produced cw **216 nm** laser light for Cu, At CLS, Katarina Preocanin, MSc SFU (2025)

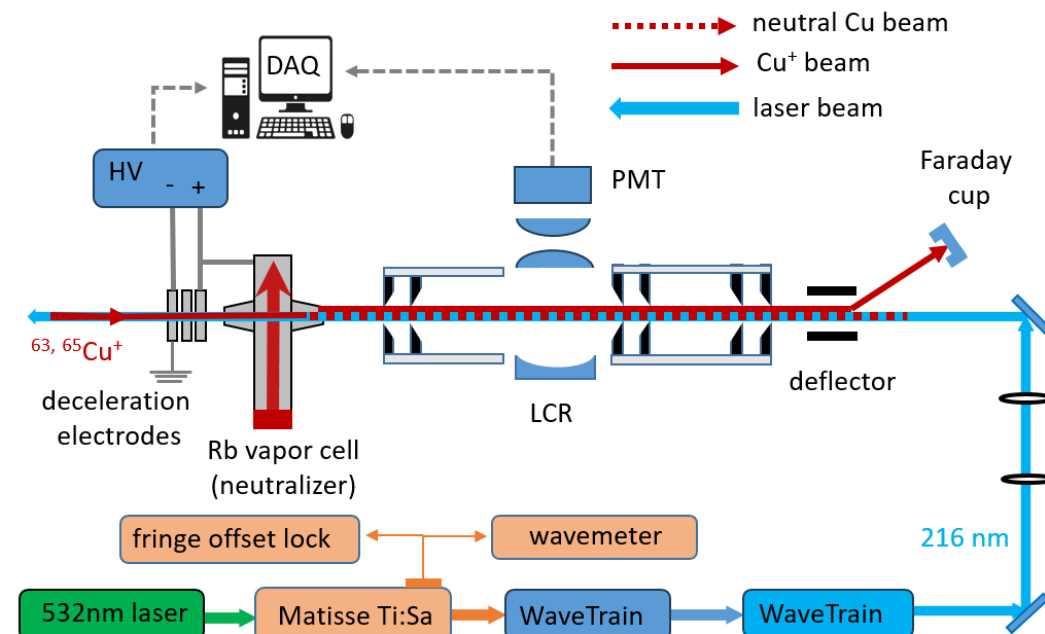
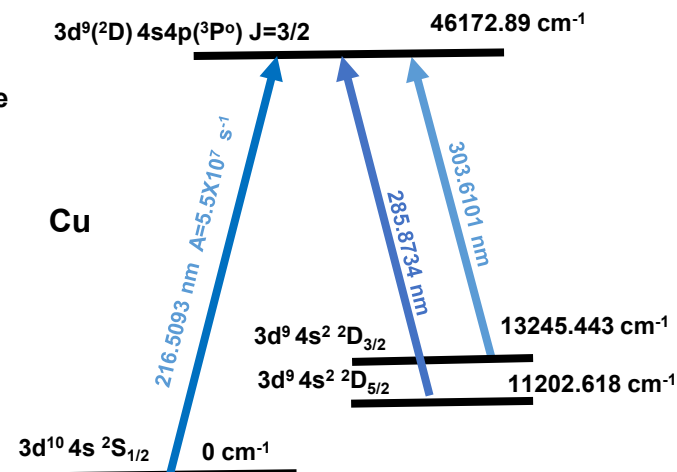
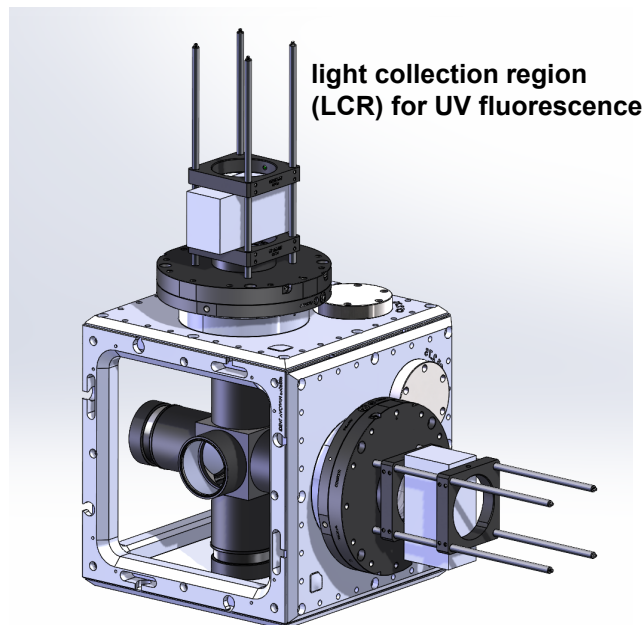


fringe offset lock



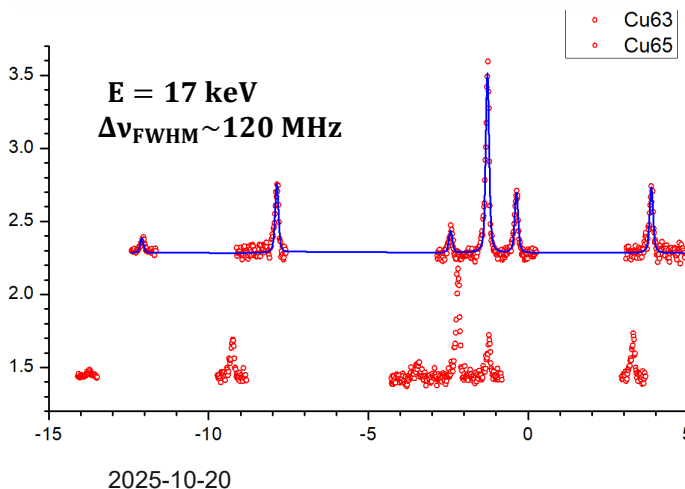
- ❑ 300 MHz free-spectral-range scanning interferometer temperature stabilized to 0.1 °C and hermetically sealed.
- ❑ major cause of laser drift is air pressure variation.
- ❑ long-term dye laser frequency stability is +/- 5 MHz, determined by the HeNe reference laser stability and scan non-linearities.

UV optical detection system for CLS
 transition wavelength = 216 nm
 OLIS stable beam $\rightarrow 1.4 \times 10^8$ atoms/s Cu



UV LCR works with detection eff. of 1.2 and 1.7E-6 per neutral Cu atom for horizontal and vertical arms, respectively, by assuming neutralized population are all at the ground state.

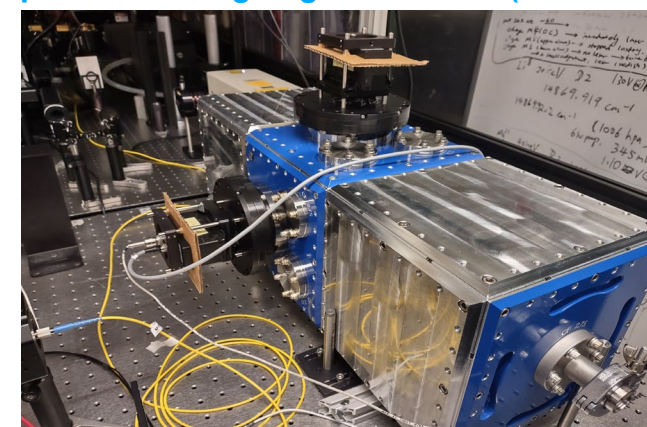
further improvement ongoing on the LCR (offline test)



Cu63,65 $2S_{1/2} \rightarrow J=3/2$ (216.5 nm)

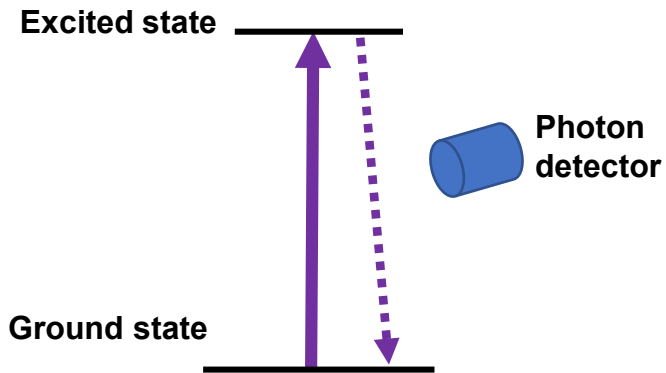
	I	A(2S _{1/2}) MHz	A(J=3/2) MHz	B(J=3/2) MHz
⁶³ Cu	3/2	5866.92(1)	2168(13)	?(?)
⁶⁵ Cu	3/2	6284.41(3.5)		?(?)

new data for A, B hyperfine constants for 216.5nm Cu transition



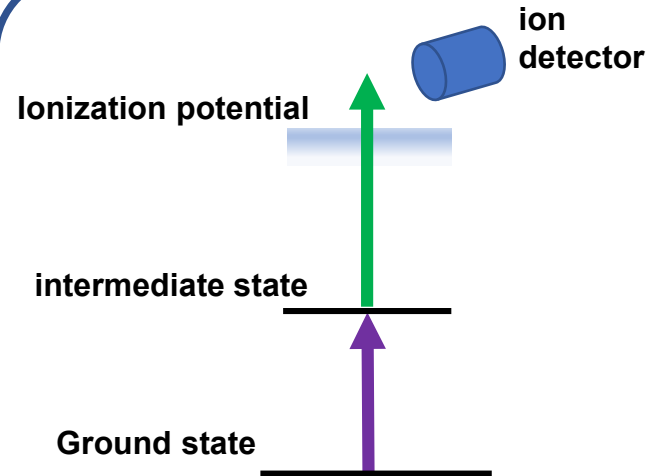
Resonance ionization spectroscopy in collinear geometry RISIKO as developed at Mainz U around 1990 and implemented at CERN-ISOLDE with CRIS around 2010, allows collinear laser spectroscopy with beam intensity as low as 20/s (^{78}Cu , R. P. de Groote et al., Phys. Rev. C 96, 041302 (2017).)

Fluorescence method



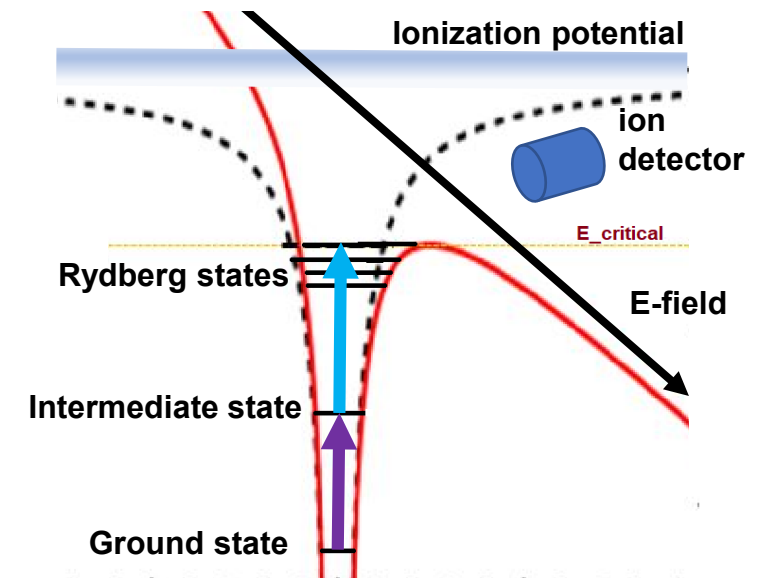
- Difficulty to collect 4π fluorescence
- Photon detection efficiency not high
- Suppress the stray light and dark counts

RISIKO & CRIS



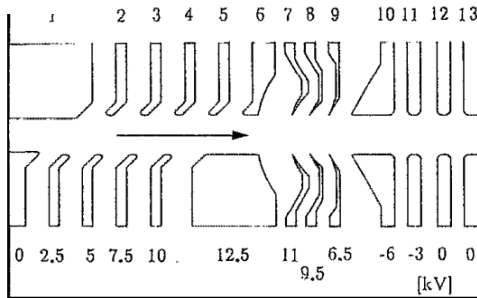
- Efficient charge particle detection (~100%)
- Nonresonant ionization needs high laser power \rightarrow pulsed laser \rightarrow bunching beam
- Background ions generated by collision with residual gas (need high vacuum to 10^{-10} mbar)

RISIKO & CRIS with Rydberg-state field ionization

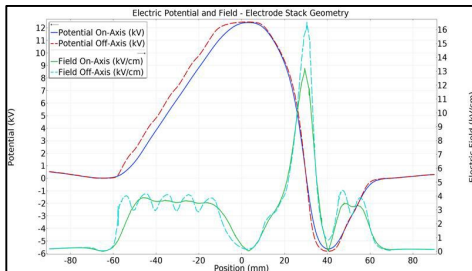
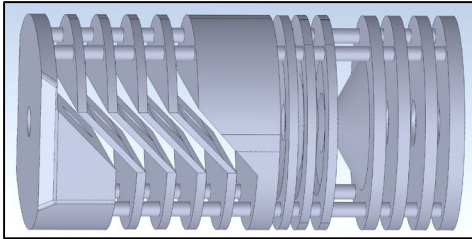


- Efficient charge particle detection (~100%)
- Efficient resonant excitation + field ionization
- Field ionizer- allow mark the energy of the beam which are generated inside \rightarrow allow the separation of the background ions and signal ions.

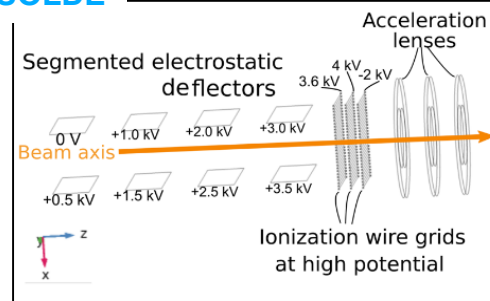
Mainz



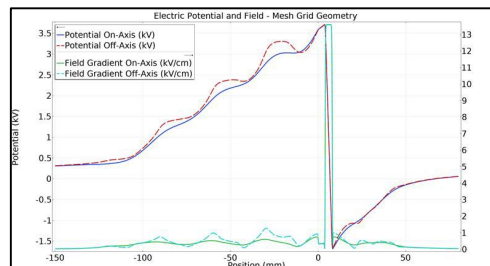
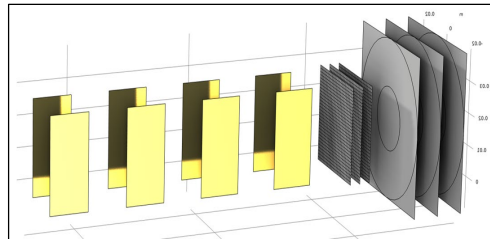
Our simulations:



ISOLDE



Our simulations:



Design Goals:

- Simulate the Mainz and ISOLDE designs using COMSOL

Mainz: K. Stratmann et al., Rev. Sci. Instrum. 65, 1847 (1994).

ISOLDE: A. R. Vernon et al., Sci. Rep. 10, 12306 (2020).

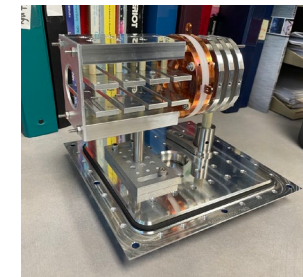
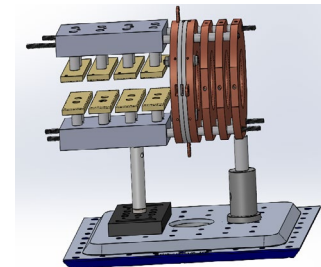
- Adapt the ISOLDE design into ISAC-polarizer

Simulation results:

Both geometries had a **gradual rise in potential** followed by a **steep drop** and a subsequent rise to ground. The sharp potential drop establishes a **localized region of high field** where Rydberg atoms are ionized.

Mainz: gradual field drop allows for Rydberg state identification through energy analysis,
ISOLDE: indiscriminate ionization with less energy spread.

Rydberg-state field ionizer based on ISOLDE has been built

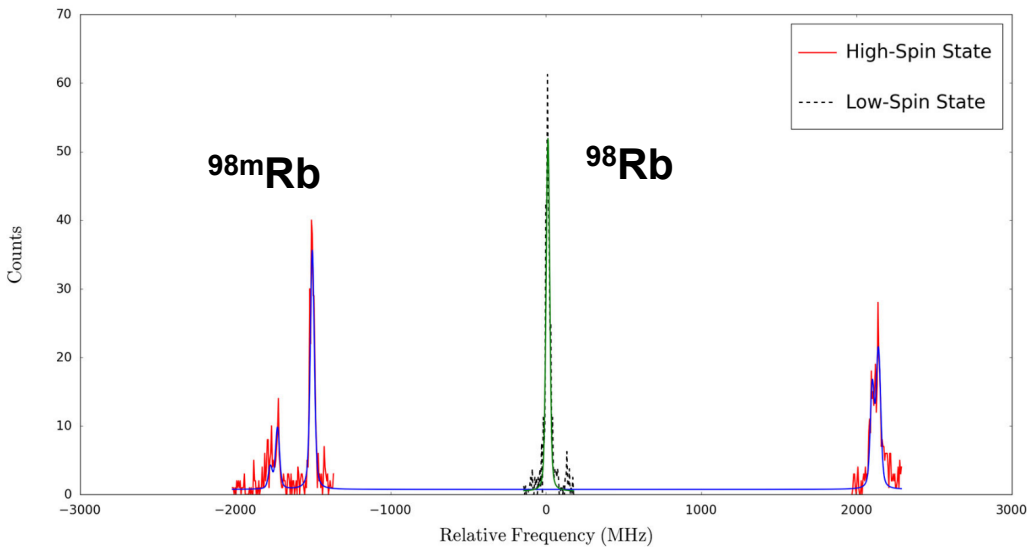


The original RISIKO field-ionizer from Mainz U will be implemented and compared to ISOLDE field-ionizer for high sensitivity collinear laser spectroscopy at TRIUMF.

implementing Rydberg-state field-ionizer will provide isomer-selected beams to OSAKA and GRIFFIN

14

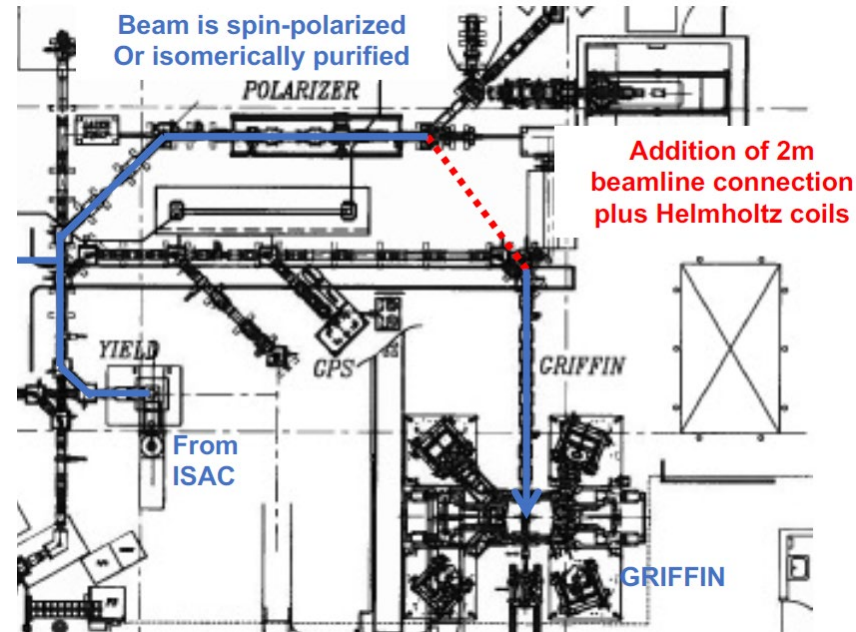
collinear resonant laser ionization allows delivery of isobar-free beams for nuclear spectroscopy



T. J. Procter, Eur. Phys. J. A (2015) 51: 23

S1475 (M. Rajabali, Tennessee Tech Uni.)

cw RIB with Rydberg-state field ionizer avoids beam bunching, while allowing background free beam delivery of isobar free, and possibly polarized beams



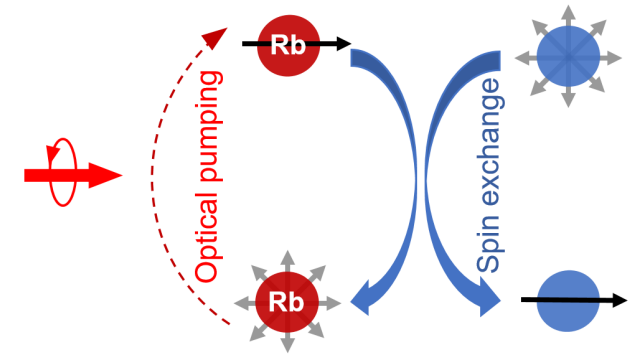
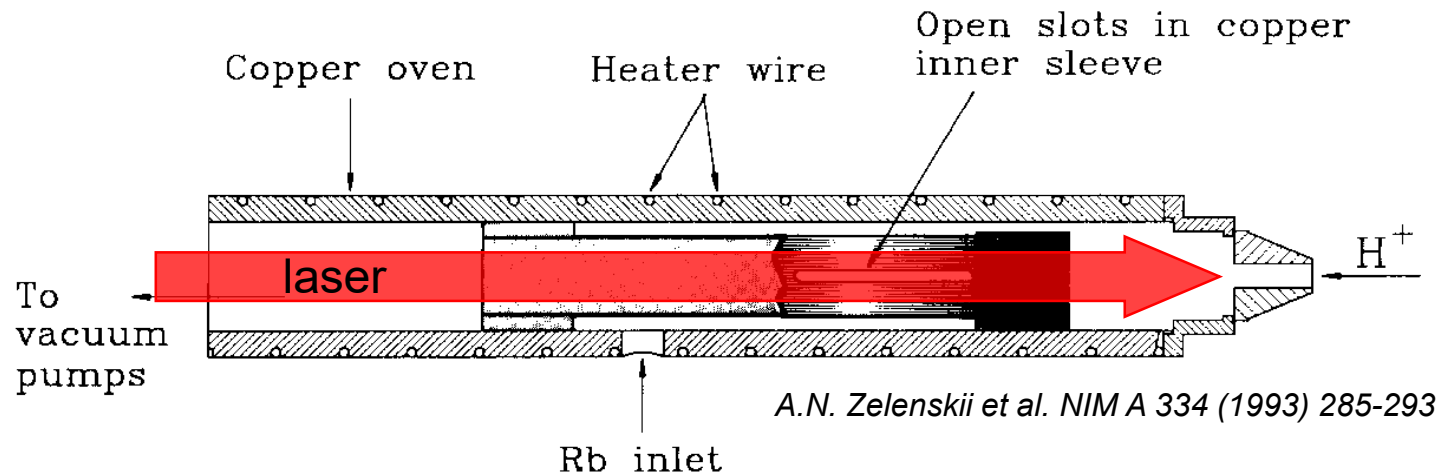
beamline extension for polarized beams to GRIFFIN spectrometer (2027)

a spin-polarized alkali-vapour mixture as a spin-exchange medium to transfer polarization to ion beams.

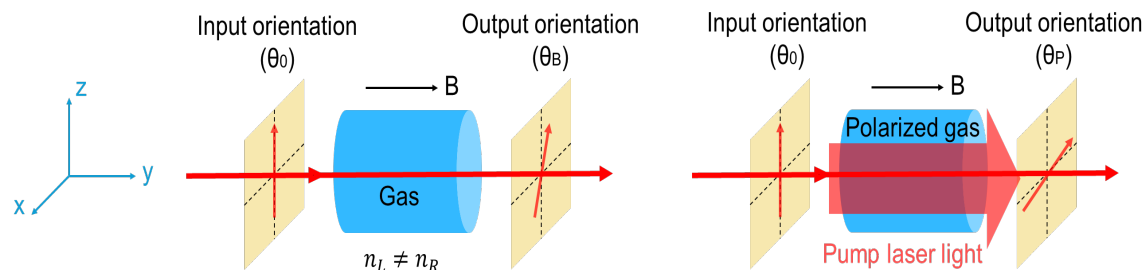
15

alkali-vapor spin-exchange cell:

- 😊 Simply and one laser setup for polarizing one alkali element.
- 😞 radiation trapping causes depolarization in dense vapor. **Possible solution:** mixture of two alkali species
- 😞 Depolarization on the cell wall. **Possible solution:** non-depolarizing wall coating

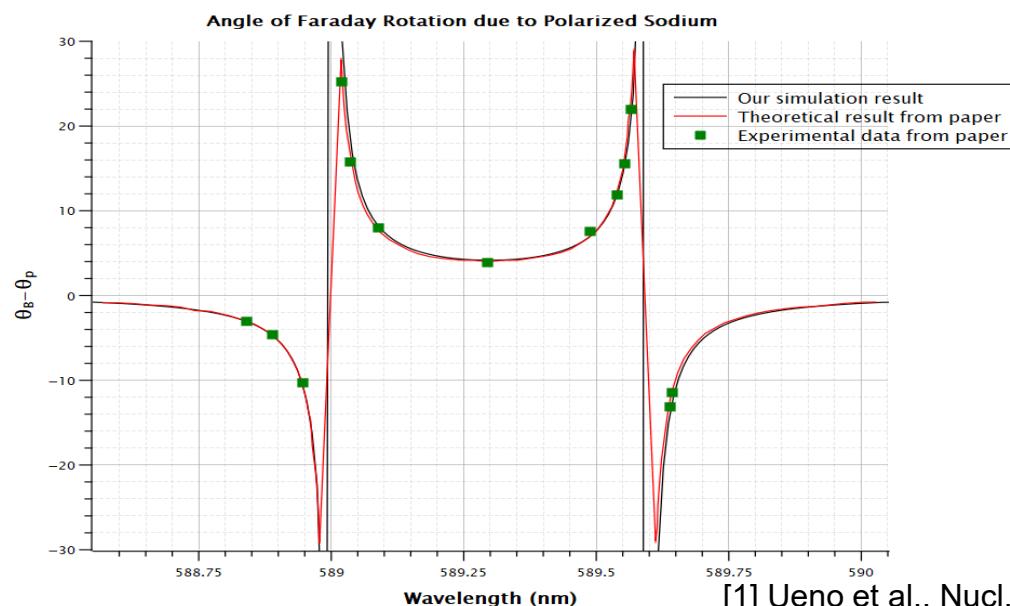


Similar configuration as the optically-pumped polarized H^- ion source designed at TRIUMF previously. H^+ passes through optically pumped Rb vapor in a neutralizer cell and picks up polarized electrons by charge exchange to form electron-polarized neutral H atoms.



$Nl = \frac{\theta_B - \theta_0}{V}$	$P = \frac{\theta_P - \theta_B}{\alpha(\theta_B - \theta_0)}$	V – Verdet constant α – alpha constant
N – atomic density (temperature dependent) l – length of interaction between gas and laser	P – spin polarization of the gas	Both constants depend on magnetic field and the wavelength of the laser.

test our numerical simulation code by comparing with Ueno et al. [1]



[1] Ueno et al., Nucl. Instrum. Meth. Phys. Res. A 262 (1987) 170

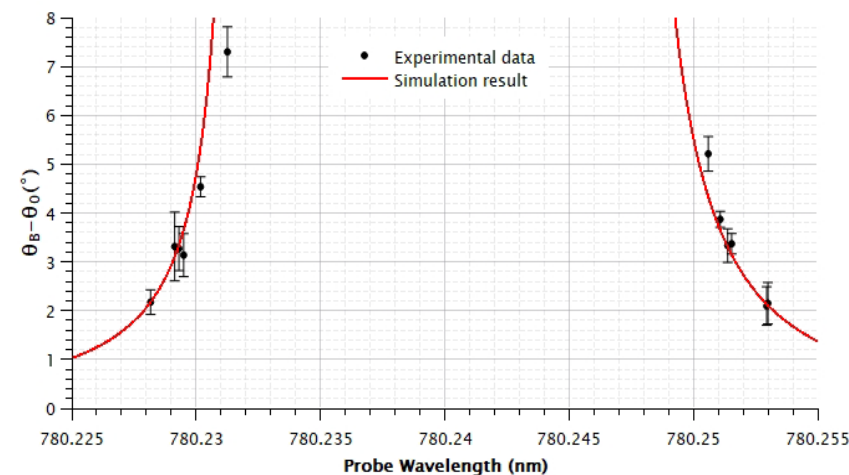
2025 Co-op student project (Simon Liu, Enzo Picinini, Anna Parker, Kenney Lai, Mehar Sahota)

16

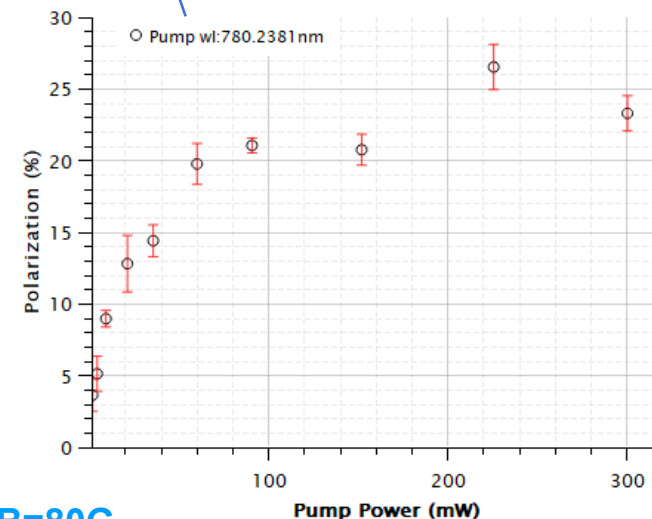
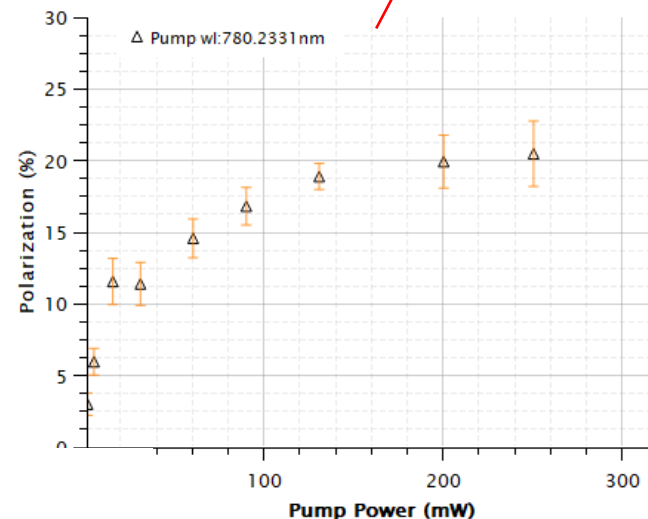
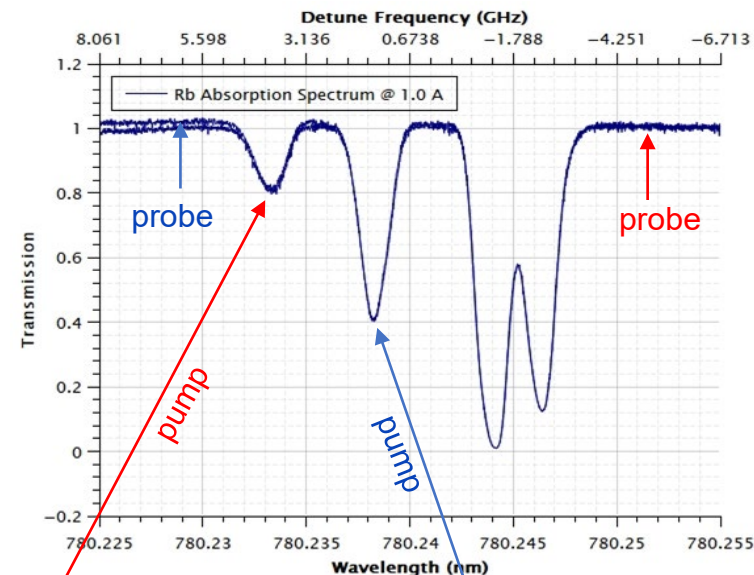
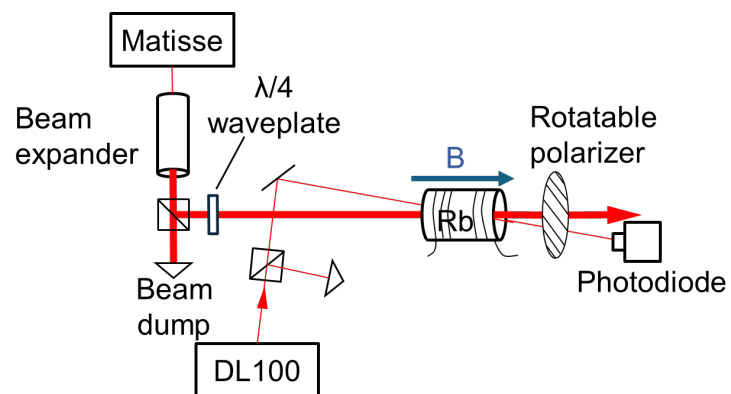
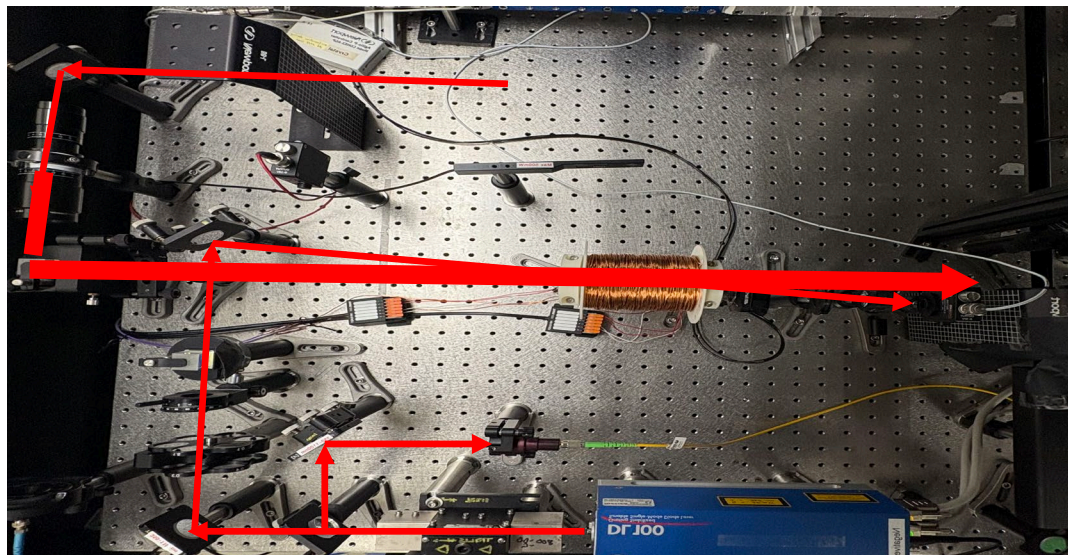
The Verdet and α constants are computed numerically over a range of magnetic fields B and wavelengths λ .

- To describe both weak- and strong-field coupling regimes, the method employs Hamiltonian matrix formalism.
- Starting from the $|LSJM_J M_I\rangle$ basis (which corresponds to the strong-field limit), the full Hamiltonian is constructed, including Zeeman and hyperfine interactions.
- The Hamiltonian is then diagonalized at each magnetic field to obtain the eigenvalues and eigenvectors, from which the transition energies and strengths—and thus the Verdet and α constants—are derived.

test our numerical simulation code by comparing with our experimental data



To match our experimental condition, for the simulation B and T is set to 120G, 53°C.



B=80G

- Matisse cw Ti:Sa laser: circularly polarized laser for pumping.
- Toptica diode laser DL100: linearly polarized laser for probing.

Thank you for your attention



Questions?

TRIUMF team:

Jens Lassen

Ruohong Li

Julius Wessolek

Graduate student

Katarina Preocanin,

Runa Yasuda (TokyoUAT)

TRIUMF Co-op students:

Mathias Roman,

Aryan Prasad, Élyse D'Aoust,

Alexia Landry, Simon Liu,

Enzo Picinini, Anna Parker,

Kenney Lai, Mehar Sahota

MITACS students:

Rahul Vasudevan,

Pratham Kulkarni,

Cristina Villasenor

We gratefully acknowledge the help & support from
TRIUMF, collaborating Universities & NSERC funding



UNIVERSITY
OF MANITOBA

